
Partial Causal Structure Learning for Valid Selective Conformal Inference under Interventions

Amir Asiaee*¹

Kaveh Aryan²

James P. Long³

¹Department of Biostatistics, Vanderbilt University Medical Center, TN 37203, USA

²Department of Informatics, King’s College London, London, UK

³Department of Biostatistics, MD Anderson Cancer Center, Houston, TX, USA

Abstract

Selective conformal prediction can yield substantially tighter uncertainty sets when we can identify calibration examples that are exchangeable with the test example. In interventional settings, such as perturbation experiments in genomics, exchangeability often holds only within subsets of interventions that leave a target variable “unaffected” (e.g., non-descendants of an intervened node in a causal graph). We study the practical regime where this invariance structure is unknown and must be learned from data. Our contributions are: (i) a *contamination-robust conformal coverage theorem* that quantifies how misclassification of “unaffected” calibration examples degrades coverage via an explicit function $g(\delta, n)$ of the contamination fraction and calibration set size, providing a finite-sample lower bound that holds for arbitrary contaminating distributions; (ii) a *task-driven partial causal learning* formulation that estimates only the binary descendant indicators $Z_{a,i} = \mathbf{1}\{i \in \text{desc}(a)\}$ needed for selective calibration, rather than the full causal graph; and (iii) *algorithms* for descendant discovery via perturbation intersection patterns (differentially affected variable set intersections across interventions), and for approximate distance-to-intervention estimation via local invariant causal prediction. We provide recovery conditions under which contamination is controlled. Experiments on synthetic linear structural equation models (SEMs) validate the bound: under controlled contamination up to $\delta = 0.30$, the corrected procedure maintains ≥ 0.95 coverage while uncorrected selective CP degrades to 0.867. A proof-of-concept on Replogle K562 CRISPR interference (CRISPRi) perturbation data demonstrates applicability to real genomic screens.

1 INTRODUCTION

Conformal prediction (CP) provides distribution-free uncertainty quantification: given any black-box predictor, CP constructs prediction sets with finite-sample marginal coverage guarantees under exchangeability [Vovk et al., 2005, Shafer and Vovk, 2008, Angelopoulos and Bates, 2023]. Split conformal prediction, in particular, requires only a single pass over a held-out calibration set and scales to modern high-dimensional problems.

However, the marginal coverage guarantee of standard CP can be loose when the data exhibit heterogeneity. In many scientific applications, data are generated under multiple interventions or environments, and exchangeability holds *only within* certain subsets of these conditions. If we can identify such subsets, *selective* (or *Mondrian*) calibration [Vovk, 2012, Boström et al., 2021] provides the same coverage guarantee but with prediction sets that are often substantially tighter, because calibration is restricted to the relevant stratum.

Motivating application: gene perturbation experiments.

Single-cell perturbation screens such as Perturb-seq [Dixit et al., 2016, Replogle et al., 2022] now routinely profile the transcriptional consequences of hundreds to thousands of genetic interventions (e.g., CRISPRi knockdowns) in a single experiment. A central scientific question is: for a given target gene i , which interventions affect its expression and by how much? Under a causal model, intervening on gene a changes the distribution of gene i if and only if i is a causal descendant of a in the gene regulatory network. For non-descendant targets, the residual distribution under intervention a is the same as under control, creating a natural exchangeability structure. Exploiting this structure via selective conformal inference can provide tighter, more informative prediction intervals for the effects of unseen interventions—enabling better prioritization in experimental design and more confident in silico differential expression calls.

*Correspondence to Amir Asiaee

<amir.asiaee@vumc.org>

The challenge is that the descendant structure is rarely known. Full causal graph learning in high dimensions is notoriously difficult and computationally expensive [Peters et al., 2017, Hauser and Bühlmann, 2012], and the resulting errors propagate to the selective calibration procedure in ways that are poorly understood. We (i) quantify the statistical cost of imperfect causal knowledge for conformal inference, and (ii) develop algorithms that learn only the partial causal structure needed for valid selective calibration.

Contributions. Our contributions are:

1. **δ -robust selective conformal coverage (Theorem 1).** We prove a finite-sample coverage lower bound for selective conformal prediction when the calibration set is contaminated by a fraction δ of misclassified interventions. The bound $\mathbb{P}(Y_i^{(a^*)} \in C) \geq 1 - \alpha - g(\delta, n)$ is explicit, distribution-free over the contaminating scores, and recovers exact $1 - \alpha$ coverage when $\delta = 0$. This result quantifies the coverage cost of misclassifying calibration strata.
2. **Task-driven partial causal learning formulation.** Rather than learning the full causal graph G , we formulate the objective as estimating binary labels $Z_{a,i} = \mathbf{1}\{i \in \text{desc}(a)\}$ for relevant intervention–target pairs. This shifts the problem from graph estimation to a structured binary classification task, where the key performance metric is the false positive rate (FPR) of declaring a non-descendant as a descendant, since FPR directly controls δ .
3. **Algorithms with recovery conditions.** We propose two complementary algorithms: (a) *Descendant discovery via perturbation intersection patterns*, which uses differentially affected variable sets across interventions (e.g., differentially expressed gene sets in genomics) and set intersections to estimate descendant sets; and (b) *Local ICP for distance estimation*, which adapts invariant causal prediction [Peters et al., 2016] to estimate a path-length-based distance $\hat{d}(a, i)$ without learning the full graph. We provide recovery conditions (Propositions 1–2) under which the algorithms control contamination.
4. **Experimental validation.** On synthetic linear SEMs with $p = 200$ nodes, we demonstrate that coverage degrades monotonically with contamination as predicted by Theorem 1 (from 0.905 to 0.867 over $\delta \in [0, 0.3]$), and that the corrected procedure empirically achieves ≥ 0.95 coverage at all nonzero contamination levels (above the nominal $1 - \alpha = 0.9$), reflecting the conservative nature of the α -correction. A real-data experiment on Replogle K562 CRISPRi data confirms that the corrected method is the only one to exceed nominal coverage on genuine perturbation screens.

Organization. Section 2 discusses related work. Section 3 formalizes the setup. Section 4 presents the δ -robustness

theorem. Section 5 formulates the task-driven learning objective. Section 6 describes the algorithms. Section 7 states recovery conditions. Section 8 details the experimental evaluation. Section 9 concludes. All proofs are deferred to the Supplementary Material.

2 RELATED WORK

Conformal prediction: foundations and efficiency. Conformal prediction originated in the algorithmic learning theory literature [Vovk et al., 2005] and has become a standard approach to distribution-free uncertainty quantification [Shafer and Vovk, 2008, Angelopoulos and Bates, 2023]. Split conformal prediction is the dominant practical variant, requiring only calibration on held-out data. Conformalized quantile regression [Romano et al., 2019] improves efficiency by adapting interval widths to the input, while maintaining the finite-sample coverage guarantee.

Conditional and Mondrian conformal prediction. Standard CP provides only marginal coverage; conditional coverage (coverage conditional on X) is generally impossible without strong assumptions [Vovk, 2012]. Mondrian conformal prediction [Boström et al., 2021] provides a practical middle ground: it stratifies calibration points into categories and applies CP within each stratum, achieving stratum-conditional coverage. Gibbs et al. [2025] develop a framework interpolating between marginal and conditional validity, showing how to achieve coverage guarantees over finite collections of subgroups. Our selective calibration is Mondrian-like, with strata defined by causal invariances rather than observable features.

Conformal prediction under distribution shift. When exchangeability fails, weighted conformal prediction can restore validity under covariate shift if the density ratio is known [Tibshirani et al., 2019]. Barber et al. [2023] develop conformal prediction beyond exchangeability, providing a general framework for weighted and non-exchangeable settings with explicit finite-sample coverage bounds. The contamination model we study is complementary: rather than a continuous distributional shift, we analyze the discrete setting where a fraction of calibration points come from the wrong stratum.

Robust conformal prediction under contamination. The robustness of conformal prediction to data corruption has received growing attention. Einbinder et al. [2024] study label noise robustness, showing that conformal prediction is conservative when noise is dispersive and providing corrections for adversarial noise of bounded size. Clarkson et al. [2024] study split conformal prediction under a Huber contamination model, providing coverage bounds in terms of the contamination fraction and the Kolmogorov–Smirnov distance. Gendler et al. [2022] address adversarial input perturbations via randomized smoothing. Our Theorem 1 is tailored to the *selective* (Mondrian) setting where contamination arises from misclassification of calibration strata,

which is the natural error mode when causal structure is learned. The key distinction is that we bound coverage loss as a function of the fraction of miscategorized calibration points, without assumptions on the contaminating distribution.

Conformal prediction and causal inference. Conformal methods have been applied to counterfactual and treatment effect inference. Lei and Candès [2021] develop conformal inference of counterfactuals and individual treatment effects in the potential outcomes framework, providing finite-sample coverage under unconfoundedness. Alaa et al. [2023] extend this to conformal meta-learners for predictive inference of individualized treatment effects. By contrast, we use causal structure to identify approximately exchangeable calibration subsets across *multiple simultaneous interventions*, enabling tighter predictive intervals for post-intervention outcomes rather than performing inference on a treatment effect.

Causal discovery from interventional data. Learning causal structure from a combination of observational and interventional data is a central problem in causal inference. Hauser and Bühlmann [2012, 2015] characterize interventional Markov equivalence classes and develop greedy algorithms for learning directed acyclic graphs (DAGs) from mixed data. Eberhardt et al. [2005] establish that $\lceil \log_2(N) \rceil + 1$ experiments suffice to identify the full causal graph over N variables in the worst case, motivating efficient experimental design. Squires et al. [2020] propose active structure learning via directed clique trees, achieving near-optimal intervention counts for full graph identification. Brouillard et al. [2020] develop differentiable causal discovery methods that scale to larger graphs using interventional data. These works all aim to recover the complete DAG; the approach here is *task-driven*, learning only the partial structure (descendant indicators $Z_{a,i}$) needed for selective conformal calibration.

Invariant causal prediction. Invariant causal prediction (ICP) [Peters et al., 2016] identifies causal parents of a target by exploiting the stability of the conditional distribution $P(Y_i | X_{\text{Pa}(i)})$ across environments. Nonlinear extensions have been developed by Heinze-Deml et al. [2018]. We adapt ICP ideas locally to estimate parent sets and thereby distance-to-intervention, without attempting full graph recovery.

Perturbation biology and causal gene networks. Single-cell perturbation screens provide a natural setting for interventional causal inference. Perturb-seq [Dixit et al., 2016] combines CRISPR perturbations with single-cell RNA-seq readouts. Replogle et al. [2022] scaled this to genome-wide screens. Peidli et al. [2024] provide harmonized perturbation datasets across studies. CausalBench [Chevalley et al., 2025] benchmarks gene network inference from perturbation data. Differential expression testing in perturbation screens raises statistical challenges, including the need for appropriate ag-

gregation and multiple testing correction [Squair et al., 2021, Barry et al., 2024]. Differentially expressed gene (DEG) sets from perturbation screens serve as the inputs for our descendant discovery algorithm (Algorithm 1).

3 SETUP: INTERVENTIONAL PREDICTION AND SELECTIVE CONFORMAL

We consider a collection of interventions (environments) indexed by $a \in \mathcal{A}$. For each intervention a we observe i.i.d. samples of outcomes $Y^{(a)} \in \mathbb{R}^p$ (e.g., gene expression vector) and possibly covariates $X^{(a)}$. Typically X represents shared sample-level information that does not depend on a (e.g., cell type, batch indicator, or technical covariates), though in some designs $X^{(a)}$ may include intervention-specific features such as dosage or timing. We focus on predicting a scalar target component $Y_i^{(a)}$ (or a derived effect size) for each $i \in [p]$.

Let $\hat{f}_i(a, X)$ be a fitted predictor of Y_i in intervention a . We use a calibration score (nonconformity score)

$$R_i^{(a)} = S_i(X^{(a)}, Y_i^{(a)}) \equiv |Y_i^{(a)} - \hat{f}_i(a, X^{(a)})|.$$

3.1 SELECTIVE INVARIANCE SETS

Suppose that for each intervention a and target i there exists an unknown indicator

$$Z_{a,i} = \mathbf{1}\{i \in \text{desc}(a)\},$$

where $\text{desc}(a)$ denotes causal descendants of a in an underlying causal graph $G = (V, E)$ (or more generally, the set of targets whose data-generating mechanism changes under a). We assume a single graph G shared across all samples; extending to covariate-dependent graphs (e.g., cell-type-specific regulatory networks) is an important direction for future work. Define the *safe set* for target i as $\mathcal{A}^*(i) = \{a \in \mathcal{A} : Z_{a,i} = 0\}$ (i.e., interventions that do not affect i). Given a test intervention a^* , the *calibration pool* is $\mathcal{A}_{\text{cal}} = \mathcal{A} \setminus \{a^*\}$.

Assumption 1 (Selective exchangeability). Fix a target gene i and a test intervention a^* with $Z_{a^*,i} = 0$ (i.e., i is unaffected by a^*). The calibration scores $\{R_i^{(a)} : a \in \mathcal{A}^*(i)\} \cup \{R_i^{(a^*)}\}$ are exchangeable.

If $Z_{a^*,i} = 0$, we can calibrate using only interventions where i is unaffected, yielding valid but tighter intervals than pooling all interventions. When $Z_{a^*,i} = 1$ (the test intervention does affect target i), selective calibration does not apply; one should instead use pooled conformal prediction over all calibration interventions, or restrict calibration to interventions that affect i through similar causal pathways. Our framework focuses on the $Z_{a^*,i} = 0$ case, where selective calibration offers the clearest gains.

Example 1 (Why selective calibration tightens intervals). Consider a gene regulatory network with 100 genes and 50

interventions. For a target gene i , suppose only 5 of the 50 interventions are ancestors of i (i.e., affect i). Pooled conformal prediction uses all 50 residuals, mixing 5 “affected” residuals (which tend to be large) with 45 “unaffected” residuals. Selective conformal uses only the 45 unaffected residuals. Since affected residuals inflate the quantile, the selective interval is tighter while maintaining exact $1 - \alpha$ coverage.

3.2 SELECTIVE SPLIT CONFORMAL INTERVAL (ORACLE)

Given a set of calibration scores $\{R_i^{(a)} : a \in \mathcal{A}^*(i)\}$ of size m , define the oracle conformal quantile

$$k = \lceil (m+1)(1-\alpha) \rceil.$$

$$\hat{q}_i^{\text{oracle}}(1-\alpha) = \text{the } k\text{-th smallest value in}$$

$$\{R_i^{(a)} : a \in \mathcal{A}^*(i)\} \cup \{\infty\}.$$

The prediction interval is

$$C_{i,1-\alpha}^{\text{oracle}}(a^*, x) = [\hat{f}_i(a^*, x) - \hat{q}_i^{\text{oracle}}(1-\alpha),$$

$$\hat{f}_i(a^*, x) + \hat{q}_i^{\text{oracle}}(1-\alpha)].$$

Under Assumption 1, this interval achieves $1 - \alpha$ marginal coverage by the standard conformal argument [Shafer and Vovk, 2008].

4 δ -ROBUSTNESS: COVERAGE UNDER CONTAMINATED SELECTIVE CALIBRATION

In practice we do not know $\mathcal{A}^*(i)$ and must estimate it. Let $\hat{\mathcal{A}}(i, a^*) \subseteq \mathcal{A}_{\text{cal}}$ (recall $\mathcal{A}_{\text{cal}} = \mathcal{A} \setminus \{a^*\}$) be the selected set of calibration interventions used for target i and test intervention a^* . Some selected interventions may violate exchangeability (misclassified as “unaffected”), contaminating the calibration scores.

Definition 1 (Contamination fraction). Let $\mathcal{A}^* = \mathcal{A}^*(i) \cap \mathcal{A}_{\text{cal}}$ be the (unknown) set of truly exchangeable calibration interventions for target i . Define the contamination fraction

$$\delta \equiv \frac{|\hat{\mathcal{A}}(i, a^*) \setminus \mathcal{A}^*|}{|\hat{\mathcal{A}}(i, a^*)|}.$$

That is, δ is the fraction of calibration interventions in the selected set that are actually *affected* (i.e., $Z_{a,i} = 1$) and therefore not exchangeable with the test score.

The selected set $\hat{\mathcal{A}}$ naturally partitions into three regions (Figure 1): *good* interventions $\hat{\mathcal{A}} \cap \mathcal{A}^*$ (m truly safe and exchangeable with a^*); *bad* interventions $\hat{\mathcal{A}} \setminus \mathcal{A}^*$ ($n - m$ contaminants that break exchangeability); and *missed* interventions $\mathcal{A}^* \setminus \hat{\mathcal{A}}$ (truly safe but not selected—wasted data that reduces calibration set size but does not harm coverage). The contamination fraction is $\delta = (n - m)/n$.

4.1 MAIN ROBUSTNESS THEOREM

We prove a finite-sample coverage lower bound that depends explicitly on δ and does *not* assume anything about the score distribution on contaminated interventions.

Theorem 1 (δ -robust selective conformal coverage). *Fix (i, a^*) with $Z_{a^*,i} = 0$, and suppose that scores from the “good” set \mathcal{A}^* are exchangeable with the test score $R_i^{(a^*)}$ (Assumption 1). Let $\hat{\mathcal{A}}$ be any selected calibration set of size $n = |\hat{\mathcal{A}}|$, and let $m = |\hat{\mathcal{A}} \cap \mathcal{A}^*|$ be the number of good calibration interventions. Construct the split conformal interval using all scores in $\hat{\mathcal{A}}$: let \hat{q} be the $\lceil (n+1)(1-\alpha) \rceil$ -th order statistic of $\{R_i^{(a)} : a \in \hat{\mathcal{A}}\}$ and output $C_{i,1-\alpha} = [\hat{f}_i \pm \hat{q}]$. Then, for all possible distributions of contaminated scores,*

$$\mathbb{P}(R_i^{(a^*)} \leq \hat{q}) \geq 1 - \alpha - \frac{n-m}{m+1}.$$

In terms of the contamination fraction $\delta = (n-m)/n$,

$$\mathbb{P}(Y_i^{(a^*)} \in C_{i,1-\alpha}) \geq 1 - \alpha - g(\delta, n),$$

$$g(\delta, n) \equiv \frac{\delta n}{(1-\delta)n+1}.$$

For large n , $g(\delta, n) \approx \delta/(1-\delta)$.

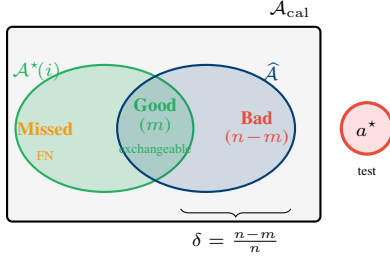
Remark 1 (Interpretation and how to use it). Theorem 1 turns structure learning error into a direct statistical price for selective inference. If δ is small, coverage is close to nominal. Moreover, the bound suggests a conservative correction: to guarantee $1 - \alpha$ coverage, run conformal with target miscoverage $\alpha' = \alpha - g(\hat{\delta}, n)$, where $\hat{\delta}$ is an upper bound on the contamination fraction. When $g(\hat{\delta}, n) \geq \alpha$ (i.e., $\alpha' \leq 0$), the correction exceeds the error budget and the interval becomes infinite, yielding trivial coverage of 1. Equivalently, one can design the learning procedure to ensure δ is below a threshold δ_{max} such that $g(\delta_{\text{max}}, n) \leq \epsilon$ for a desired slack ϵ .

Remark 2 (Comparison with Huber contamination bounds). Clarkson et al. [2024] study split conformal prediction under a Huber contamination model where an ϵ -fraction of *all* calibration points are corrupted. Our setting is structurally different: contamination arises specifically from misclassification of the Mondrian stratum, and the contamination fraction δ is specific to each (i, a^*) pair. This makes δ a quantity that the learner can control through the design of the classification procedure. The resulting bound is tighter than applying a generic Huber bound because it exploits the selective calibration structure.

Remark 3 (Benign contamination). In many perturbation applications, interventions misclassified as “unaffected” will actually induce *larger* residuals (because the intervention does change the target), making \hat{q} larger and the interval conservative. Theorem 1 is worst-case over contaminating distributions; empirical coverage is often better than the bound.

Corollary 1 (Corrected selective conformal). *If $\hat{\delta}$ is an upper bound on the contamination fraction δ (possibly estimated or given by the recovery conditions of Propositions 1–2), then running split conformal with nominal level $\alpha' = \alpha - g(\hat{\delta}, n)$ yields coverage at least $1 - \alpha$ for the selective interval (when $\alpha' \leq 0$, the interval is $(-\infty, \infty)$ and coverage is trivially 1).*

(a) Partition of calibration interventions



(b) Concrete example on a causal DAG

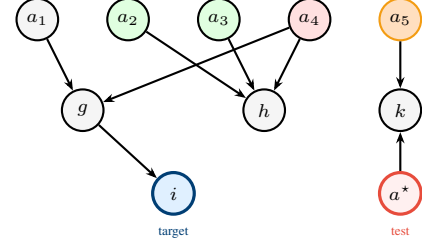


Figure 1: Anatomy of the intervention sets for target gene i . (a) The calibration pool \mathcal{A}_{cal} (rectangle) contains all interventions except the test a^* . The safe set $\mathcal{A}^*(i)$ (green ellipse) consists of interventions that do not affect i ; the selected set $\hat{\mathcal{A}}$ (blue ellipse) is our classifier’s estimate of $\mathcal{A}^*(i)$. Their overlap produces three regions: **good** (selected and truly safe; m exchangeable scores), **bad** (selected but actually affecting i ; $n-m$ contaminants that degrade coverage by $g(\delta, n)$), and **missed** (truly safe but not selected; reduces n but does not harm coverage). (b) Example DAG with five calibration interventions and target gene i . $\text{desc}(a_1) = \{g, i\}$, $\text{desc}(a_4) = \{g, h, i\}$ (both affect i); $\text{desc}(a_2) = \{h\}$, $\text{desc}(a_3) = \{h\}$, $\text{desc}(a_5) = \{k\}$ (safe for i). The classifier selects $\hat{\mathcal{A}} = \{a_2, a_3, a_4\}$: a_2, a_3 are **good**, a_4 is **bad** (FP, $\delta = 1/3$), and a_5 is **missed** (FN).

5 TASK-DRIVEN PARTIAL CAUSAL LEARNING

Theorem 1 implies that we do *not* need to perfectly learn the full causal graph. We need a procedure that makes δ small for the calibration sets we actually use. This motivates a *task-driven* formulation.

5.1 BINARY CLASSIFICATION VIEW

For each intervention a and target i , we estimate

$$\hat{Z}_{a,i} \approx Z_{a,i} = \mathbf{1}\{i \in \text{desc}(a)\}.$$

We then select calibration interventions for (i, a^*) as

$$\hat{\mathcal{A}}(i, a^*) = \{a \in \mathcal{A}_{\text{cal}} : \hat{Z}_{a,i} = 0\},$$

possibly intersected with other constraints (same cell type/context, similar batch, etc.).

5.2 FROM CLASSIFIER ERRORS TO CONTAMINATION

Let π_0 be the fraction of truly unaffected interventions in \mathcal{A}_{cal} for target i . Let FPR_i be the fraction of truly affected calibration interventions that are misclassified as unaffected, and let FNR_i (false-negative rate) be the fraction of truly unaffected calibration interventions that are misclassified as affected. Then

$$\delta = \frac{(1 - \pi_0)\text{FPR}_i}{\pi_0(1 - \text{FNR}_i) + (1 - \pi_0)\text{FPR}_i}.$$

This expression shows that *controlling the false positive rate* FPR_i is *critical*. A classifier that conservatively labels borderline cases as “affected” (accepting higher FNR_i , which reduces the calibration set size) is preferable to one that aggressively labels cases as “unaffected” (low FNR_i but higher FPR_i , which increases contamination).

Remark 4 (Asymmetric error costs). In sparse networks, most interventions do not affect a given target (π_0 is large), so even a moderate FPR_i can lead to small δ . Indeed, when π_0 is sufficiently large, a naive strategy of labeling *all* calibration interventions as “unaffected” (i.e., $\text{FPR}_i = 1$,

$\text{FNR}_i = 0$) yields $\delta = (1 - \pi_0)/1 = 1 - \pi_0$; for example, with $\pi_0 \geq 0.95$ this gives $\delta \leq 0.053$, requiring no learning algorithm at all. Algorithm 1 improves upon this baseline by further reducing δ while maintaining calibration set size. However, δ grows rapidly with FPR_i when π_0 is small (dense networks or hub genes). The task-driven formulation makes this tradeoff explicit and motivates conservative classification strategies.

5.3 REDUCTION IN COMPLEXITY

Full causal graph learning over p variables requires estimating $O(p^2)$ edge parameters (or $O(2^p)$ DAG structures in the worst case). The task-driven objective reduces this to estimating $|\mathcal{A}| \times p$ binary labels, and in practice only a small fraction of these are needed (those for which the corresponding (a^*, i) pairs will be queried at test time). Furthermore, the labels $Z_{a,i}$ have combinatorial structure that can be exploited: if $a \rightarrow b \rightarrow c$ in G , then $Z_{a,c} = 1$ and $Z_{b,c} = 1$, enabling information sharing across interventions.

6 ALGORITHMS

We present two practical estimators for $\hat{Z}_{a,i}$ and $\hat{d}(a, i)$ from interventional data. Both are designed for scalability in high dimensions and many interventions.

6.1 DESCENDANT DISCOVERY VIA PERTURBATION INTERSECTION PATTERNS

The first algorithm estimates descendant sets $\widehat{\text{desc}}(a)$ from differentially affected variable sets across interventions, using set intersections to prune false positives.

Input: differentially affected sets. Assume we have a differentially affected set $\mathcal{S}_a \subset [p]$ for each intervention $a \in \mathcal{A}$ —that is, an estimate of the variables whose distribution changes under a . In genomics these are differentially expressed gene (DEG) sets, computed by standard statistical tests (e.g., two-sample t -tests or Wilcoxon rank-

Algorithm 1 Descendant Discovery via Differentially Affected Set Intersections

Require: Differentially affected sets $\{\mathcal{S}_a\}_{a \in \mathcal{A}}$, interventions \mathcal{A}

Ensure: Estimated descendant sets $\{\widehat{\text{desc}}(a)\}_{a \in \mathcal{A}}$

```
1: for each intervention  $a \in \mathcal{A}$  do
2:    $\mathcal{U}(a) \leftarrow \{b \in \mathcal{A} : a \in \mathcal{S}_b\}$  {Upstream interventions of  $a$ }

3:   if  $\mathcal{U}(a) = \emptyset$  then
4:      $\text{Cand}(a) \leftarrow \mathcal{S}_a$  {Fallback to own affected set}
5:   else
6:      $\text{Cand}(a) \leftarrow \mathcal{S}_a \cap \bigcap_{b \in \mathcal{U}(a)} \mathcal{S}_b$  {Intersection with up-
       stream affected sets}
7:   end if
8:    $\widehat{\text{desc}}(a) \leftarrow \text{Cand}(a)$ 
9: end for
10: return  $\{\widehat{\text{desc}}(a)\}_{a \in \mathcal{A}}$ 
```

sum tests with Benjamini–Hochberg correction [Squair et al., 2021, Barry et al., 2024]); in other domains any test for distributional change applies. \mathcal{S}_a is an estimate of $\{i : Z_{a,i} = 1\} = \text{desc}(a)$, but may contain false positives and false negatives.

Intersection estimator. For each intervention a , identify interventions that are “upstream” of a (i.e., interventions b such that a is affected by b):

$$\mathcal{U}(a) = \{b \in \mathcal{A} : a \in \mathcal{S}_b\}.$$

We estimate the descendant set of a by intersecting its own affected set with those of its upstream interventions:

$$\widehat{\text{desc}}(a) = \begin{cases} \mathcal{S}_a, & \mathcal{U}(a) = \emptyset, \\ \mathcal{S}_a \cap \bigcap_{b \in \mathcal{U}(a)} \mathcal{S}_b, & \text{otherwise.} \end{cases}$$

The intuition is: if b is upstream of a (i.e., $a \in \text{desc}(b)$), then every descendant of a is also a descendant of b , so $\text{desc}(a) \subseteq \text{desc}(b)$. Thus descendants of a should appear consistently across \mathcal{S}_a and across upstream affected sets, while spurious entries will not. Equivalently, one can view this as starting from \mathcal{S}_a and pruning any candidate variable that fails to appear in some upstream affected set; we present the set-intersection form for clarity.

Complexity. Algorithm 1 runs in $O(|\mathcal{A}|^2 \cdot p)$ time in the worst case (for each of $|\mathcal{A}|$ interventions, iterating over $O(|\mathcal{A}|)$ upstream interventions and $O(p)$ candidate genes). In practice, the estimator is implemented with set operations; since affected sets are typically sparse, the intersections are much cheaper than the worst-case bound.

6.2 LOCAL ICP FOR DISTANCE ESTIMATION

Beyond binary descendant labels, selective inference can benefit from a *distance-to-intervention* notion $\hat{d}(a, i)$ that prioritizes closer calibration interventions or enables weighted conformal calibration. We propose a local search inspired by ICP [Peters et al., 2016] that traces back from the target i through estimated parents to obtain a coarse path-length estimate $\hat{d}(a, i)$ without learning the full graph. The full algorithm (Algorithm 2) and details on using distance for kernel-weighted calibration are given in the Supplemen-

tary Material.

7 CONDITIONS FOR RECOVERY

This section states concrete, checkable conditions under which Algorithm 1 controls the contamination fraction δ .

Assumption 2 (Interventional faithfulness and detectability). There is an underlying causal DAG $G = (V, E)$ such that intervening on node a changes (in distribution) precisely the descendants of a —i.e., for every $i \in \text{desc}(a)$ the marginal $P(Y_i | \text{do}(a))$ differs from $P(Y_i)$ (no path cancellations), and for every $i \notin \text{desc}(a)$ it is unchanged. Moreover, each descendant effect is detectable with probability at least $1 - \epsilon_{\text{fn}}$ by the testing procedure used to form \mathcal{S}_a . Formally: for each $a \in \mathcal{A}$ and $i \in \text{desc}(a)$, $\mathbb{P}(i \in \mathcal{S}_a) \geq 1 - \epsilon_{\text{fn}}$, and for each $i \notin \text{desc}(a)$, $\mathbb{P}(i \in \mathcal{S}_a) \leq \epsilon_{\text{fp}}$.

Proposition 1 (Intersection candidates are supersets). *Under Assumption 2, for any intervention $a \in \mathcal{A}$, if $\mathcal{U}(a) \neq \emptyset$ and for every $b \in \mathcal{U}(a)$ we have $a \in \text{desc}(b)$ (i.e., all identified upstream interventions are true ancestors), then with probability at least $1 - |\text{desc}(a)| \cdot (|\mathcal{U}(a)| + 1) \cdot \epsilon_{\text{fn}}$ (by a union bound),*

$$\text{desc}(a) \subseteq \text{Cand}(a).$$

Assumption 3 (Upstream diversity for intersections). For any intervention $a \in \mathcal{A}$ and non-descendant $i \notin \text{desc}(a)$, there exists an intervention $b \in \mathcal{A}$ such that $a \in \text{desc}(b)$ but $i \notin \text{desc}(b)$. Moreover, for such a b the testing procedure satisfies $\mathbb{P}(a \in \mathcal{S}_b \text{ and } i \notin \mathcal{S}_b) \geq 1 - \epsilon_{\text{cx}}$.

Assumption 3 requires “upstream diversity”: for each non-descendant i , there exists an ancestor of a whose descendants include a but not i . This is plausible when ancestors of a have sufficiently diverse descendant sets.

Proposition 2 (False positive control via upstream intersections). *Under Assumptions 2–3, for any non-descendant $i \notin \text{desc}(a)$, the intersection estimator in Algorithm 1 excludes i with probability at least $1 - \epsilon_{\text{cx}}$. Consequently, the false positive rate for $\hat{Z}_{a,i}$ satisfies*

$$\mathbb{P}(\hat{Z}_{a,i} = 1 \mid Z_{a,i} = 0) \leq \epsilon_{\text{cx}}.$$

Corollary 2 (Contamination control via recovery conditions). *Under Assumptions 2–3, the expected contamination fraction for target i and the calibration set $\hat{\mathcal{A}}(i, a^*)$ satisfies*

$$\mathbb{E}[\delta] \leq \frac{(1 - \pi_0)\epsilon_{\text{cx}}}{\pi_0(1 - \bar{u}\epsilon_{\text{fn}}) + (1 - \pi_0)\epsilon_{\text{cx}}},$$

where π_0 is the fraction of calibration interventions that are unaffected for target i and $\bar{u} = \max_a |\mathcal{U}(a)|$ is the maximum upstream set size across interventions. In sparse networks where π_0 is near 1 and ϵ_{cx} is small, $\mathbb{E}[\delta]$ is small.

Together, Propositions 1–2 and Corollary 2 imply a tunable tradeoff between missed descendants (which reduce calibration set size but do not violate coverage) and spurious descendants (which contaminate the calibration set), directly controlling the coverage loss via Theorem 1.

8 EXPERIMENTS

We evaluate the framework on synthetic and real data, focusing on three questions: (Q1) Does selective conformal prediction with learned \hat{Z} maintain valid coverage? (Q2) Does coverage degrade with contamination δ as predicted by Theorem 1? (Q3) Does the corrected procedure (Corollary 1) restore nominal coverage?

Throughout, *Coverage* denotes the empirical fraction of test points whose true outcome falls within the prediction interval, and *Width* denotes the average interval length across test points. Both are computed over all (test intervention, target gene) pairs in the held-out test set.

8.1 SYNTHETIC INTERVENTIONAL SEM

Setup. We generate random DAGs using the Erdős–Rényi model on $p = 200$ nodes with expected degree $d_{\text{avg}} = 2.0$. Edge weights are sampled uniformly from $[-1, -0.3] \cup [0.3, 1]$. The linear Gaussian SEM is $V = B^\top V + \varepsilon$ with $\varepsilon \sim \mathcal{N}(0, I)$, where $V \in \mathbb{R}^p$ is the vector of all node values (we use V here to avoid confusion with the covariates X from Section 3). Interventions are hard (do-operator), setting $V_a := 0$. We use $n_{\text{obs}} = 200$ observational and $n_a = 200$ interventional samples per node, with $|\mathcal{A}| = 150$ randomly selected intervention targets. Ground-truth descendant sets $\text{desc}(a)$ are computed from the transitive closure of B .

Conformal scores. In practice, $\hat{f}_i(a, X)$ could be any predictor of Y_i under intervention a —for example, the per-intervention sample mean $\hat{f}_i(a) = \bar{Y}_i^{(a)}$, or a regression model trained on unaffected interventions—and the non-conformity scores would be the resulting residuals $R_i^{(a)} = |Y_i^{(a)} - \hat{f}_i(a, X^{(a)})|$. To isolate the effect of calibration set selection from predictor quality, we use synthetic scores in this experiment: unaffected pairs ($Z_{a,i} = 0$) receive scores $R_i^{(a)} = |N(0, 1)|$ and affected pairs ($Z_{a,i} = 1$) receive $R_i^{(a)} = |N(0, 0.15)|$. This models a setting where contaminating the calibration set with affected scores (which are systematically smaller) pulls the conformal quantile downward, causing under-coverage for test points with genuinely unaffected (larger) residuals.

DEG procedure and descendant estimation. For each intervention a , gene-wise two-sample t -tests comparing interventional vs. observational data with Benjamini–Hochberg correction at $q = 0.05$ yield DEG sets \mathcal{S}_a . Algorithm 1 is applied to obtain $\hat{Z}_{a,i}$. Interventions are split into 10% training, 81% calibration, and 9% test. We fit \hat{Z} using only the training and calibration interventions (holding out test interventions from descendant discovery), and evaluate coverage on the held-out test interventions using calibration interventions for conformal calibration. Note that the conformal scores (synthetic $|N(0, \sigma)|$) are generated independently of the DEG-based descendant estimation, so the selection of $\hat{\mathcal{A}}$ does not introduce dependence between \hat{Z} and the calibration scores.

Table 1: Main synthetic experiment ($p = 200$, $|\mathcal{A}| = 150$, $\alpha = 0.1$). Coverage and width averaged over 20 seeds. All methods achieve 0% infinite-width intervals.

Method	Coverage	Width	n_{cal}	$\hat{\delta}$
Oracle	0.901	3.35	118.8	0.000
Estimated	0.899	3.32	121.0	0.018
Pooled	0.899	3.32	121.0	0.000
Corrected	0.918	3.58	121.0	0.018

Results. Table 1 summarizes results over 20 random seeds (220,132 evaluations). All four methods achieve coverage near the nominal $1 - \alpha = 0.9$ level. The estimated contamination from Algorithm 1 is very low ($\hat{\delta} = 0.018$), indicating that the intersection-based procedure keeps contamination well-controlled in the linear SEM setting. Because π_0 is high in this sparse network (most interventions are unaffected for a given target), the learned selector labels nearly all calibration interventions as unaffected, so $\hat{\mathcal{A}} \approx \mathcal{A}_{\text{cal}}$ and the Estimated and Pooled methods coincide; their differences emerge under controlled contamination (Section 8.2). Corrected selective CP is slightly conservative (coverage 0.918) with 8% wider intervals, reflecting the cost of the α -correction even when contamination is small.

8.2 CONTROLLED δ ABLATION

To directly test Theorem 1, we inject controlled contamination. Starting from the true unaffected calibration set, we replace a target fraction $\delta_{\text{inject}} \in \{0, 0.05, 0.1, 0.15, 0.2, 0.3\}$ of scores with affected-gene scores (resampled from truly affected calibration points with replacement to ensure the target contamination rate is achieved). We use $p = 200$ nodes, $|\mathcal{A}| = 150$ interventions, and repeat over 100 random seeds (1,065,408 total evaluations).

Results. Figure 2 shows the results (full numerical breakdown in Table 3 in the Supplementary Material). Estimated coverage degrades monotonically from 0.905 at $\delta = 0$ to 0.867 at $\delta = 0.30$, confirming that contamination of the selective calibration set causes under-coverage as predicted by Theorem 1. The Corrected method empirically achieves coverage ≥ 0.95 at all nonzero contamination levels ($\delta \geq 0.05$), well above the nominal 0.9, at the cost of 1.2–1.8 \times wider intervals. Oracle and Pooled coverage remain flat across δ values, as expected. The empirical coverage always exceeds the theoretical lower bound $1 - \alpha - g(\delta, n)$ (Figure 3 in the Supplementary Material), confirming the bound is valid.

8.3 REAL PERTURBATION DATA: REPLOGLE K562 CRISPRi SCREEN

We apply the complete method to real data from the Replogle K562 CRISPRi genome-scale screen [Replogle et al., 2022], accessed via Zenodo. We select the 50 perturbations with the largest cell counts (≥ 200 cells each), retaining $p \approx 5,000$ genes expressed in $\geq 10\%$ of cells. Log-fold-change (LFC) vectors are computed per perturbation against the non-targeting control. Since ground-truth descendant

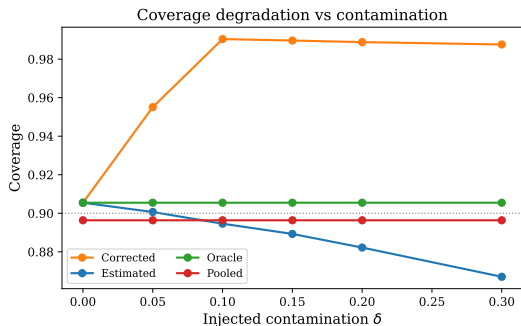


Figure 2: Coverage vs. injected contamination δ . Estimated (blue) degrades monotonically from 0.905 to 0.867; Corrected (orange) remains above 0.95 for $\delta \geq 0.05$; Oracle (green) and Pooled (red) are unaffected. Dashed line: nominal $1 - \alpha = 0.9$.

Table 2: Real-data results on Replogle K562 CRISPRi screen. Coverage and width averaged over 5 test perturbations (Corrected: over feasible evaluations only). Corrected is the only method above nominal, but is feasible for 60% of evaluations.

Method	Coverage	Width	n_{cal}	Feasible
Oracle (proxy)	0.864	0.306	36.7	100%
Estimated	0.888	0.349	40.0	100%
Pooled	0.888	0.349	40.0	100%
Corrected	0.906	0.329	40.0	59.8%

sets are unavailable, we define proxy ‘‘oracle’’ affected sets as the top 10% of genes by absolute LFC per perturbation, and DEG sets analogously. Perturbations are split into 10% training, 81% calibration, and 9% test (5 test perturbations, ~ 40 calibration perturbations). We fit \hat{Z} using only the training and calibration perturbations (holding out test perturbations from descendant discovery), and evaluate coverage on the held-out test perturbations using calibration perturbations for conformal calibration.

Results. Table 2 summarizes results over 90,000 evaluations. The Corrected method is the only one achieving coverage above the nominal 0.9 level (0.906, averaged over feasible evaluations only), consistent with the theory. However, it is feasible (finite quantile) for only 59.8% of evaluations; the remaining 40.2% produce infinite intervals because the corrected α' is too stringent for the available calibration set size ($n_{\text{cal}} \approx 40$). The proxy oracle achieves only 0.864 coverage, reflecting genuine exchangeability violations in real perturbation data: some perturbations (e.g., *tim23b*, coverage 0.60; *bcr*, coverage 0.74) exhibit strong off-target or indirect effects that violate the assumption that ‘‘unaffected’’ genes have exchangeable residuals. Bootstrap stability analysis (100 replicates) confirms low variance: coverage standard deviations ≤ 0.003 for all methods.

Limitations of the real-data evaluation. The proxy oracle is constructed from LFC quantiles, not from true causal knowledge. Its coverage shortfall (0.864 vs. the nominal 0.9) indicates that the LFC-based proxy does not perfectly capture the exchangeability structure, likely because (i) indirect

downstream effects create correlated residuals even among ‘‘unaffected’’ genes, and (ii) batch effects and technical noise break the i.i.d. assumption within strata. Despite these violations, the qualitative ordering of methods—Corrected $>$ Estimated \approx Pooled $>$ Oracle—is consistent with the theoretical predictions, and the Corrected method is the only one to exceed nominal coverage. As in the synthetic experiment, the Estimated and Pooled results coincide because the learned selector classifies nearly all calibration perturbations as unaffected given the high sparsity of the proxy descendant structure. A more thorough real-data evaluation with larger calibration sets (more perturbations) and biologically validated oracle sets remains open.

9 DISCUSSION

Selective conformal inference can tighten uncertainty quantification in interventional problems when exchangeable calibration subsets can be identified. Our δ -robustness theorem (Theorem 1) provides an explicit, finite-sample bound linking causal structure learning accuracy to inferential validity: the coverage loss is bounded by $g(\delta, n) = \delta n / ((1 - \delta)n + 1)$, which is small when the contamination fraction is small.

The controlled δ ablation (Section 8.2) validates this prediction empirically: Estimated selective CP coverage degrades monotonically from 0.905 to 0.867 as contamination increases from 0 to 30%, while the Corrected procedure empirically achieves ≥ 0.95 coverage at all nonzero contamination levels, at the cost of 1.2–1.8 \times wider intervals. The theoretical bound is satisfied at every contamination level tested. On the Replogle K562 CRISPRi real-data experiment (Section 8.3), the Corrected method is the only one to exceed nominal coverage (0.906), though it is feasible for only 60% of evaluations due to the stringent α -correction with limited calibration data ($n_{\text{cal}} \approx 40$). The proxy oracle’s sub-nominal coverage (0.864) highlights the difficulty of defining ground-truth exchangeability in real perturbation biology, where indirect effects and batch artifacts create residual correlations that violate i.i.d. assumptions.

Several directions remain open. First, the bound in Theorem 1 is worst-case over contaminating distributions; tighter bounds may be achievable under benign contamination models (e.g., when affected interventions produce stochastically larger residuals), which our experiments suggest is common in practice (the bound gap grows with δ). Second, a natural extension is a more thorough theoretical analysis of the local ICP distance estimator (Algorithm 2), including conditions for consistent distance estimation and its effect on weighted conformal coverage. Third, larger-scale real-data evaluations with more calibration perturbations and biologically validated oracle sets would strengthen the empirical case and improve Corrected method feasibility. Finally, combining the task-driven approach with active experimental design for causal discovery [Squires et al., 2020, Eberhardt et al., 2005] could lead to efficient sequential strategies that minimize the number of perturbation experiments needed to achieve a desired coverage guarantee.

References

- Ahmed M. Alaa, Zaid Ahmad, and Mark van der Laan. Conformal meta-learners for predictive inference of individual treatment effects. In *Advances in Neural Information Processing Systems (NeurIPS)*, 2023.
- Anastasios N. Angelopoulos and Stephen Bates. Conformal prediction: A gentle introduction. *Foundations and Trends in Machine Learning*, 16(4):494–591, 2023. doi: 10.1561/2200000101.
- Rina Foygel Barber, Emmanuel J. Candès, Aaditya Ramdas, and Ryan J. Tibshirani. Conformal prediction beyond exchangeability. *The Annals of Statistics*, 51(2):816–845, 2023. doi: 10.1214/23-AOS2276.
- Timothy Barry, Kaishu Mason, Kathryn Roeder, and Eugene Katsevich. Robust differential expression testing for single-cell CRISPR screens at low multiplicity of infection. *Genome Biology*, 25(1):124, 2024. doi: 10.1186/s13059-024-03254-2.
- Henrik Boström, Ulf Johansson, and Tuwe Löfström. Mondrian conformal predictive distributions. In *Conformal and Probabilistic Prediction and Applications (COPA)*, volume 152 of *Proceedings of Machine Learning Research*, pages 24–38, 2021.
- Philippe Brouillard, Sébastien Lachapelle, Alexandre Lacoste, Simon Lacoste-Julien, and Alexandre Drouin. Differentiable causal discovery from interventional data. In *Advances in Neural Information Processing Systems (NeurIPS)*, volume 33, 2020.
- Mathieu Chevalley, Yusuf H. Roohani, Arash Mehrjou, Jure Leskovec, and Patrick Schwab. A large-scale benchmark for network inference from single-cell perturbation data. *Communications Biology*, 8(1):412, 2025. doi: 10.1038/s42003-025-07764-y.
- Jase Clarkson, Wenkai Xu, Mihai Cucuringu, and Gesine Reinert. Split conformal prediction under data contamination. In *Conformal and Probabilistic Prediction and Applications (COPA)*, volume 230 of *Proceedings of Machine Learning Research*, 2024.
- Anshul Dixit, Oren Parnas, Bo Li, et al. Perturb-seq: Dissecting molecular circuits with scalable single-cell RNA profiling of pooled genetic screens. *Cell*, 167(7):1853–1866.e17, 2016. doi: 10.1016/j.cell.2016.11.038.
- Frederick Eberhardt, Clark Glymour, and Richard Scheines. On the number of experiments sufficient and in the worst case necessary to identify all causal relations among N variables. In *Proceedings of the 21st Conference on Uncertainty in Artificial Intelligence (UAI)*, pages 178–184, 2005.
- Bat-Sheva Einbinder, Shai Feldman, Stephen Bates, Anastasios N. Angelopoulos, Asaf Gendler, and Yaniv Romano. Label noise robustness of conformal prediction. *Journal of Machine Learning Research*, 25(1):1–66, 2024.
- Asaf Gendler, Tsui-Wei Weng, Luca Daniel, and Yaniv Romano. Adversarially robust conformal prediction. In *International Conference on Learning Representations (ICLR)*, 2022.
- Isaac Gibbs, John J. Cherian, and Emmanuel J. Candès. Conformal prediction with conditional guarantees. *Journal of the Royal Statistical Society Series B: Statistical Methodology*, 87(4):1100–1126, 2025. doi: 10.1093/jrsssb/qqaf008.
- Alain Hauser and Peter Bühlmann. Characterization and greedy learning of interventional Markov equivalence classes of directed acyclic graphs. *Journal of Machine Learning Research*, 13:2409–2464, 2012.
- Alain Hauser and Peter Bühlmann. Jointly interventional and observational data: Estimation of interventional Markov equivalence classes of directed acyclic graphs. *Journal of the Royal Statistical Society: Series B (Statistical Methodology)*, 77(1):291–318, 2015. doi: 10.1111/rssb.12071.
- Christian Heinze-Deml, Jonas Peters, and Nicolai Meinshausen. Invariant causal prediction for nonlinear models. *Journal of Causal Inference*, 6(2), 2018. doi: 10.1515/jci-2017-0016.
- Lihua Lei and Emmanuel J. Candès. Conformal inference of counterfactuals and individual treatment effects. *Journal of the Royal Statistical Society: Series B (Statistical Methodology)*, 83(5):911–938, 2021. doi: 10.1111/rssb.12445.
- Stefan Peidli, Tessa D. Green, Ciyue Shen, et al. scPerturb: Harmonized single-cell perturbation data. *Nature Methods*, 21(3):531–540, 2024. doi: 10.1038/s41592-023-02144-y.
- Jonas Peters, Peter Bühlmann, and Nicolai Meinshausen. Causal inference by using invariant prediction: Identification and confidence intervals. *Journal of the Royal Statistical Society: Series B (Statistical Methodology)*, 78(5):947–1012, 2016. doi: 10.1111/rssb.12167.
- Jonas Peters, Dominik Janzing, and Bernhard Schölkopf. *Elements of Causal Inference: Foundations and Learning Algorithms*. MIT Press, 2017.
- Joseph M. Replogle, Ryan A. Saunders, Arianne N. Pogson, et al. Mapping information-rich genotype-phenotype landscapes with genome-scale Perturb-seq. *Cell*, 185(14):2559–2575.e28, 2022. doi: 10.1016/j.cell.2022.05.013.

Yaniv Romano, Evan Patterson, and Emmanuel J. Candès. Conformalized quantile regression. In *Advances in Neural Information Processing Systems (NeurIPS)*, volume 32, 2019.

Glenn Shafer and Vladimir Vovk. A tutorial on conformal prediction. *Journal of Machine Learning Research*, 9 (Mar):371–421, 2008.

Jordan W. Squair, Matthieu Gautier, Claudia Kathe, et al. Confronting false discoveries in single-cell differential expression. *Nature Communications*, 12:5692, 2021. doi: 10.1038/s41467-021-25960-2.

Chandler Squires, Sara Magliacane, Kristjan Greenewald, Dmitriy Katz, Murat Kocaoglu, and Karthikeyan Shanmugam. Active structure learning of causal DAGs via directed clique trees. In *Advances in Neural Information Processing Systems (NeurIPS)*, volume 33, 2020.

Ryan J. Tibshirani, Rina Foygel Barber, Emmanuel J. Candès, and Aaditya Ramdas. Conformal prediction under covariate shift. In *Advances in Neural Information Processing Systems (NeurIPS)*, volume 32, 2019.

Vladimir Vovk. Conditional validity of inductive conformal predictors. In *Proceedings of the Asian Conference on Machine Learning (ACML)*, volume 25 of *Proceedings of Machine Learning Research*, pages 475–490, 2012.

Vladimir Vovk, Alex Gammerman, and Glenn Shafer. *Algorithmic Learning in a Random World*. Springer, New York, NY, 2005.

Partial Causal Structure Learning for Valid Selective Conformal Inference under Interventions

(Supplementary Material)

Amir Asiaee^{*1}

Kaveh Aryan²

James P. Long³

A ADDITIONAL EXPERIMENTAL RESULTS

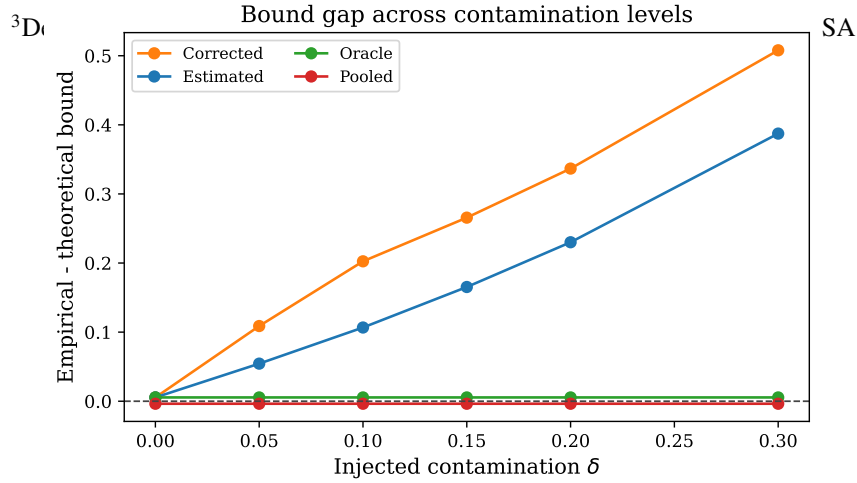


Figure 3: Gap between empirical coverage and the theoretical lower bound from Theorem 1. All values are non-negative for the selective methods (Oracle, Estimated, Corrected), confirming the bound is valid. Pooled shows a small negative gap (≈ -0.004) because it uses all calibration points without selection, so the selective coverage theorem does not apply. The gap grows with δ because worst-case adversarial contamination does not occur in practice.

Table 3: Controlled δ ablation. Coverage and width by injected contamination level. Corrected maintains ≥ 0.95 coverage at all nonzero contamination levels ($\delta \geq 0.05$). Oracle and Pooled widths (constant at 3.38 and 3.32 respectively) are omitted.

Method	δ_{inject}					
	0.00	0.05	0.10	0.15	0.20	0.30
<i>Coverage</i>						
Oracle	.905	.905	.905	.905	.905	.905
Estimated	.905	.901	.895	.889	.882	.867
Pooled	.896	.896	.896	.896	.896	.896
Corrected	.905	.955	.990	.990	.989	.988
<i>Width</i>						
Estimated	3.38	3.33	3.28	3.22	3.16	3.03
Corrected	3.38	4.09	5.52	5.48	5.44	5.35

B ALGORITHM 2: LOCAL ICP FOR DISTANCE ESTIMATION

The ICP subroutine works as follows: for a target gene g and candidate parent pool $\mathcal{P}_0^{(g)}$, test subsets $S \subseteq \mathcal{P}_0^{(g)}$ for invariance of the regression residual $Y_g - \hat{\beta}_S^T X_S$ across environments (interventions), and return a minimal invariant set as $\widehat{\text{Pa}}(g)$. The

^{*}Correspondence to Amir Asiaee <amir.asiaeetaheri@vumc.org>.

^{*}Correspondence to Amir Asiaee <amir.asiaeetaheri@vumc.org>.

Algorithm 2 Local ICP for Distance Estimation

Require: Target gene i , interventions \mathcal{A} , data $\{Y^{(a)}\}_{a \in \mathcal{A}}$, maximum depth D

Ensure: Estimated distance $\widehat{d}(a, i)$ for each $a \in \mathcal{A}$

```
1:  $\mathcal{P}_0 \leftarrow$  candidate parent pool via correlation screening or prior network
2:  $\widehat{\text{Pa}}(i) \leftarrow \text{ICP}(i, \mathcal{P}_0, \mathcal{A})$  {Invariant parent set}
3:  $\mathcal{B}_0 \leftarrow \{i\}$ 
4: for  $t = 1, \dots, D$  do
5:    $\mathcal{B}_t \leftarrow \mathcal{B}_{t-1}$ 
6:    $\{\mathcal{B}_{-1} = \emptyset\}$ 
7:   for each  $g \in \mathcal{B}_{t-1} \setminus \mathcal{B}_{t-2}$  do
8:      $\mathcal{P}_0^{(g)} \leftarrow$  candidate parent pool for  $g$ 
9:      $\widehat{\text{Pa}}(g) \leftarrow \text{ICP}(g, \mathcal{P}_0^{(g)}, \mathcal{A})$ 
10:     $\mathcal{B}_t \leftarrow \mathcal{B}_t \cup \widehat{\text{Pa}}(g)$ 
11:   end for
12: end for
13: for each  $a \in \mathcal{A}$  do
14:    $\widehat{d}(a, i) \leftarrow \min\{t : a \in \mathcal{B}_t\}$   $\{\infty$  if  $a \notin \mathcal{B}_D\}$ 
15: end for
16: return  $\{\widehat{d}(a, i)\}_{a \in \mathcal{A}}$ 
```

frontier expansion traces back from i through estimated parents, yielding a coarse path-length estimate without learning the full graph.

Using distance for weighted calibration. Given distance estimates $\widehat{d}(a, i)$, one can define weighted conformal calibration:

$$w(a) = K\left(\frac{\widehat{d}(a, i)}{h}\right),$$

where K is a kernel function and h is a bandwidth parameter. This provides a smooth interpolation between selective calibration (hard thresholding on \widehat{Z}) and pooled calibration, potentially improving efficiency when the binary classification is uncertain.

C PROOF OF THEOREM 1

Proof of Theorem 1. Setup. Fix target i and test intervention a^* with $Z_{a^*, i} = 0$. Let $\widehat{\mathcal{A}}$ be the selected calibration set of size n . Partition $\widehat{\mathcal{A}}$ into $G = \widehat{\mathcal{A}} \cap \mathcal{A}^*$ (good, $|G| = m$) and $B = \widehat{\mathcal{A}} \setminus \mathcal{A}^*$ (bad, $|B| = n - m$). Let $k = \lceil (n + 1)(1 - \alpha) \rceil$ and let \hat{q} be the k -th order statistic of all n calibration scores.

Step 1 (Worst-case bad scores). The adversary controls the values of the $n - m$ bad scores. To minimize \hat{q} (and hence minimize coverage), the adversary places all bad scores at $-\infty$. Then the bottom $n - m$ positions in the sorted order are occupied by bad scores, so

$$\hat{q} \geq R_{k-(n-m)}^G,$$

where $R_1^G \leq \dots \leq R_m^G$ are the good score order statistics. (If $k - (n - m) \leq 0$, then $\hat{q} \geq -\infty$, which is trivially true; if $k - (n - m) > m$, then $\hat{q} \geq \infty$, and coverage is 1.)

Step 2 (Exchangeability of good scores). The $m + 1$ values $\{R_1^G, \dots, R_m^G, R_i^{(a^*)}\}$ are exchangeable by Assumption 1. By the fundamental property of exchangeable sequences (see Shafer and Vovk [2008, Lemma 1] or Vovk et al. [2005, Proposition 1]), the test score $R_i^{(a^*)}$ is equally likely to occupy any of the $m + 1$ ranks among these values. Therefore, for any integer $1 \leq r \leq m$,

$$\mathbb{P}(R_i^{(a^*)} \leq R_r^G) \geq \frac{r}{m + 1}.$$

Step 3 (Combining). Setting $r = k - (n - m)$ (assuming $1 \leq r \leq m$; the bound is trivial otherwise):

$$\mathbb{P}(R_i^{(a^*)} \leq \hat{q}) \geq \mathbb{P}(R_i^{(a^*)} \leq R_r^G) \geq \frac{k - (n - m)}{m + 1}.$$

Step 4 (Algebra). Since $k = \lceil (n+1)(1-\alpha) \rceil \geq (n+1)(1-\alpha)$:

$$\begin{aligned} \frac{k - (n-m)}{m+1} &\geq \frac{(n+1)(1-\alpha) - (n-m)}{m+1} \\ &= \frac{m+1 - (n+1)\alpha}{m+1} \\ &= 1 - \frac{(n+1)\alpha}{m+1}. \end{aligned}$$

The coverage gap beyond $1 - \alpha$ is:

$$\begin{aligned} 1 - \frac{(n+1)\alpha}{m+1} - (1-\alpha) &= \alpha - \frac{(n+1)\alpha}{m+1} \\ &= \alpha \left(1 - \frac{n+1}{m+1} \right) \\ &= -\alpha \cdot \frac{n-m}{m+1}. \end{aligned}$$

Since $\alpha \leq 1$, we bound $\alpha \cdot \frac{n-m}{m+1} \leq \frac{n-m}{m+1}$, giving

$$\mathbb{P}(R_i^{(a^*)} \leq \hat{q}) \geq 1 - \alpha - \frac{n-m}{m+1}.$$

Substituting $n-m = \delta n$ and $m = (1-\delta)n$:

$$\frac{n-m}{m+1} = \frac{\delta n}{(1-\delta)n+1} = g(\delta, n). \quad \square$$

Tightness. The bound is tight in the following sense: for any δ, n, α , there exist score distributions (with the bad scores placed adversarially at $-\infty$) such that the coverage equals exactly $\frac{k-(n-m)}{m+1}$, which matches the lower bound up to the ceiling in k .

D PROOF OF COROLLARY 1

Proof. By Theorem 1 applied with nominal level α' , coverage is at least

$$\mathbb{P}(\dots) \geq 1 - \alpha' - g(\delta, n).$$

Since $\delta \leq \hat{\delta}$ and $g(\delta, n)$ is nondecreasing in δ , we have $g(\delta, n) \leq g(\hat{\delta}, n)$, hence

$$\begin{aligned} \mathbb{P}(\dots) &\geq 1 - \alpha' - g(\hat{\delta}, n) \\ &= 1 - (\alpha - g(\hat{\delta}, n)) - g(\hat{\delta}, n) \\ &= 1 - \alpha. \end{aligned} \quad \square$$

E PROOF OF PROPOSITIONS 1 AND 2

Proof of Proposition 1. Fix $a \in \mathcal{A}$ and a true descendant $i \in \text{desc}(a)$. We need $i \in \text{Cand}(a) = \mathcal{S}_a \cap \bigcap_{b \in \mathcal{U}(a)} \mathcal{S}_b$.

By Assumption 2, $\mathbb{P}(i \in \mathcal{S}_a) \geq 1 - \epsilon_{\text{fn}}$, hence $\mathbb{P}(i \notin \mathcal{S}_a) \leq \epsilon_{\text{fn}}$.

For each $b \in \mathcal{U}(a)$: if b is a true ancestor of a (i.e., $a \in \text{desc}(b)$), then $\text{desc}(a) \subseteq \text{desc}(b)$, so $i \in \text{desc}(b)$. By Assumption 2, $\mathbb{P}(i \in \mathcal{S}_b) \geq 1 - \epsilon_{\text{fn}}$, hence $\mathbb{P}(i \notin \mathcal{S}_b) \leq \epsilon_{\text{fn}}$.

The event $\{i \notin \text{Cand}(a)\}$ requires either $i \notin \mathcal{S}_a$ or $\exists b \in \mathcal{U}(a)$ with $i \notin \mathcal{S}_b$. By a union bound:

$$\mathbb{P}(i \notin \text{Cand}(a)) \leq (|\mathcal{U}(a)| + 1) \cdot \epsilon_{\text{fn}}.$$

A further union bound over all $|\text{desc}(a)|$ true descendants gives the result. Let $E_a = \{\exists i \in \text{desc}(a) : i \notin \text{Cand}(a)\}$.

$$\mathbb{P}(E_a) \leq |\text{desc}(a)| \cdot (|\mathcal{U}(a)| + 1) \cdot \epsilon_{\text{fn}}.$$

Hence $\text{desc}(a) \subseteq \text{Cand}(a)$ with probability at least $1 - |\text{desc}(a)| \cdot (|\mathcal{U}(a)| + 1) \cdot \epsilon_{\text{fn}}$. □

Proof of Proposition 2. Fix $a \in \mathcal{A}$ and $i \notin \text{desc}(a)$. By Assumption 3, there exists $b \in \mathcal{A}$ such that $a \in \text{desc}(b)$ but $i \notin \text{desc}(b)$ and

$$\mathbb{P}(a \in \mathcal{S}_b \text{ and } i \notin \mathcal{S}_b) \geq 1 - \epsilon_{\text{cx}}.$$

On this event, b is identified as upstream of a (since $a \in \mathcal{S}_b$), but $i \notin \mathcal{S}_b$. Thus $i \notin \bigcap_{b' \in \mathcal{U}(a)} \mathcal{S}_{b'}$ and therefore $i \notin \text{Cand}(a)$. Hence $\mathbb{P}(i \in \text{Cand}(a)) \leq \epsilon_{\text{cx}}$, and since $\widehat{Z}_{a,i} = \mathbf{1}\{i \in \widehat{\text{desc}}(a)\}$ where $\widehat{\text{desc}}(a) = \text{Cand}(a)$,

$$\begin{aligned} \mathbb{P}(\widehat{Z}_{a,i} = 1 \mid Z_{a,i} = 0) &= \mathbb{P}(i \in \widehat{\text{desc}}(a) \mid i \notin \text{desc}(a)) \\ &\leq \epsilon_{\text{cx}}. \end{aligned}$$

□